

Nonlinear Collective Excitations for a Periodic Array of Domain Walls in Garnet Films with Perpendicular Anisotropy

Nicolas Vukadinovic^{1,*} and Jamal Ben Youssef²

¹Dassault Aviation, 78 quai Marcel Dassault, 92552 St-Cloud, France

²Lab-STICC, CNRS/UMR 6285, Université de Bretagne Occidentale, 29285 Brest, France

Abstract. The microwave power dependence of the collective translational domain wall resonance spectra in garnet films with a perpendicular anisotropy supporting parallel stripe domains has been investigated using broadband ferromagnetic resonance experiments. Besides the fundamental domain wall resonances, a narrow subharmonic resonance at half the frequency of the fundamental Bloch domain wall resonance is revealed. For each domain wall resonance, the power dependences of the resonance frequency, the resonance linewidth and the amplitude of the power absorption at resonance have been studied. The narrow subharmonic domain wall resonance appears from a moderate input microwave power far below the values for the saturation of the fundamental domain wall resonances and its amplitude at resonance follows a nearly quadratic dependence on the microwave power. An analytical model based on the nonlinear Slonczewski's equation for the domain wall dynamics serves as a guide to justify the existence of such a subharmonic domain wall resonance and highlights the effect of an oblique pumping field configuration in accordance to our experimental setup.

1 Introduction

The parallel stripe domain pattern with up and down magnetized domains separated by thin domain walls (DWs) can be viewed as an ideal system to study the high-frequency magnetic excitations. Focusing on magnetic films with a large perpendicular anisotropy ($Q > 1$, where Q is the so-called quality factor defined as $Q = K_u/2\pi M_s^2$, where K_u is the uniaxial perpendicular anisotropy constant and M_s the saturation magnetization), a rich variety of phenomena were revealed over the past decades. When the parallel stripe domain system is excited by a uniform small-amplitude pumping field (linear regime), the acoustic and optical domain mode resonances, and the translational DW resonances are experimentally detected depending on the orientation of the pumping field with respect to stripe domain direction [1]. Regarding the translational DW resonance modes, only the collective modes with the wave vector $k=0$ are directly excited. Due to the alternate chirality between successive DWs within the array, the $k=0$ modes correspond to a uniform displacement along the DW normal for the DWs with the same chirality and, consequently, they possess an optical character. Multiple uniform translational DW resonances have been experimentally evidenced that correspond to DW modes where the DW displacement varies along the film thickness (flexural DW modes)[2]. This series of modes result from the twisted DW structure existing even in high- Q thin films with a Bloch character at the film center and a Néel character at the film surfaces. On the other hand, it was theoretically predicted in the early

1960s that the linear excitation spectrum of a single Bloch DW comprises also precessional modes termed DW spin waves (DWSWs) in addition to the translational DW modes [3, 4]. The characteristics of such DWSWs have been recently investigated by micromagnetic simulations both for a single Bloch DW and for a finite array of Bloch DWs [5]. The obtained results show nonreciprocity effects for the DWSW propagation and the possibility of unidirectional spin-wave channeling along the DWs that could be exploited for designing future diodelike spin-wave devices in the magnonics framework [6]. This brief overview relies on the linear magnetic excitations within a stripe domain pattern.

By increasing the amplitude of the pumping field or equivalently the input microwave power, new effects appear. Restricting to the domain mode resonances and the translational DW resonances, the lowest-order nonlinear process takes place in the weakly nonlinear regime characterized by a frequency shift (redshift) of the resonance lines accompanied with an asymmetric line broadening. These effects have been experimentally observed both for the domain mode resonances [7] and for the lowest-frequency DW mode resonance [8, 9]. In addition, it has been recently shown that a correct description of the power dependences of the resonance shift and the line broadening in a phenomenological approach requires to take into account a nonlinear damping parameter [7, 9]. Further increasing the amplitude of the pumping field results in a possible parametric excitation of DW waves with $k \neq 0$ through a three-DW-wave interaction mechanism (equivalent to the first-order Suhl instability for the ferromagnetic resonance (FMR) [10]) or

*e-mail: nicolas.vukadinovic@dassault-aviation.com

a four-DW-wave interaction process (second-order Suhl instability for the FMR [10]) as theoretically analyzed [11] and revealed using a magneto-optic detection [12]. Lastly, J. C. Slonczewski stated theoretically [13] that a direct excitation of DW modes, namely without any mediating pumping mode, is also possible provided to apply a rf exciting field at twice the resonance frequency of the DW mode to be excited, along the direction of the mean magnetization inside the DW, and with a magnitude exceeding a threshold value. This mechanism resembles the parallel pumping scheme in the FMR reported in the early sixties for bulk samples [14] and more recently for magnetic micro- and nanostructures [15, 16]. However, no experimental evidence of such a process has been reported, up to now, to our knowledge.

In this paper, we investigate in detail the direct excitation of multiple nonlinear translational DW resonances in single-crystal garnet films with parallel stripe domains by means of broadband FMR measurements. The DW absorption spectra have been measured for increasing values of the input microwave power. In addition to the fundamental translational DW resonances, a subharmonic DW excitation, termed hereafter 1/2 subharmonic Bloch DW resonance, is observed from intermediate microwave power levels at $f_0/2$ where f_0 is the resonance frequency of the fundamental Bloch DW mode. For each DW resonance, the power dependences of the resonance frequency, the resonance linewidth and the amplitude of the power absorption at resonance were measured. The nonlinear Slonczewski's equations were used to justify the existence of such a subharmonic DW resonance and point out the critical role played by an oblique pumping field configuration.

2 Materials and experimental procedures

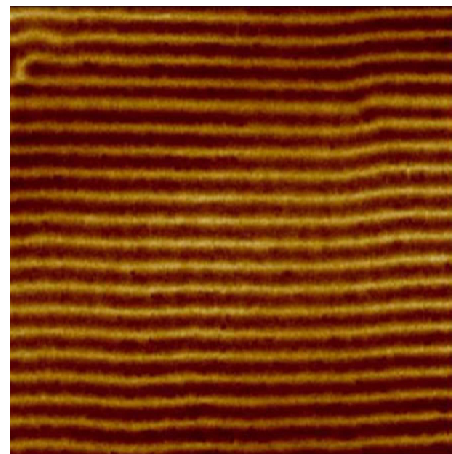
The used sample is a single-crystal bubble garnet film of composition $Y_{1.8}Bi_{0.63}Lu_{0.56}Fe_{4.06}Al_{0.83}O_{12}$ grown by liquid phase epitaxy on a Gadolinium Gallium Garnet (GGG) substrate. The film thickness is $0.66 \mu\text{m}$. The main magnetic parameters experimentally determined from vibrating sample magnetometer (VSM) and FMR measurements are the following: the saturation induction $4\pi M_s = 500 \text{ G}$, the uniaxial perpendicular anisotropy constant $K_u = 1.8 \times 10^4 \text{ erg/cm}^3$ ($Q = 1.8$), the gyromagnetic ratio $\gamma = 1.78 \times 10^7 \text{ s}^{-1} \text{ Oe}^{-1}$, and the Gilbert damping constant $\alpha = 2 \times 10^{-3}$. The exchange constant A was inferred from a theoretical law [17], namely, $A = 2.10^{-7} \text{ erg/cm}$.

The parallel stripe domain pattern was nucleated using a demagnetizing process under both perpendicular and parallel magnetic fields [18]. The zero-field stripe domain period P_0 measured by microscopy force magnetic imaging (Fig. 1(a)) is equal to $1.8 \mu\text{m}$.

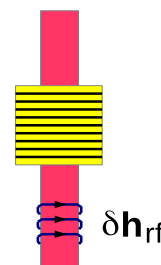
The DW resonance spectra were measured at zero-field by sweeping the frequency from 50 MHz up to 500 MHz using a broadband resonance spectrometer with a nonresonant microstrip transmission line. The input microwave power essentially ranged from 10^{-1} mW (linear regime) up to 200 mW. The input signal was then sent through a

high-pass filter ($\geq 200 \text{ MHz}$) to eliminate any subharmonics before exciting the sample. The frequency scanning rate was fixed at 0.25 MHz/s . The selected pumping field orientation (Fig.1 (b)). corresponds to the predominant in-plane component of the rf exciting field being parallel to the stripe domain direction. The small out-of-plane component of the rf exciting field is along the film normal. Some additional measurements were carried out in the presence of a DC magnetic field H_x applied along the stripe domain direction (Fig.1 (c)) for a fixed input microwave power $P = 30 \text{ mW}$.

(a)



(b)



(c)

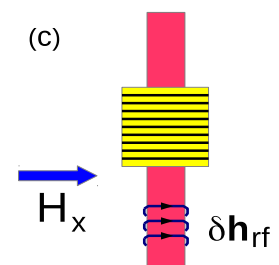


Figure 1. (a) Zero-field magnetic force microscopy (MFM) image of the parallel stripe domains for the studied garnet film with perpendicular anisotropy. The image size is $30 \mu\text{m} \times 30 \mu\text{m}$. Sketch of the experimental pumping field configurations without (b) and with (c) a DC magnetic field applied along the stripe domain direction (x-axis). The in-plane component of the exciting magnetic field δh_{rf} is parallel to the stripe domain direction.

3 Experimental results

3.1 Nonlinear DW resonance spectra

3.1.1 Zero-field spectra

The experimental zero-field DW resonance spectra recorded for three values of the input microwave power are displayed in Fig. 2. The low-level power spectrum ($P = 10^{-1} \text{ mW}$, linear regime) reveals two well-defined

resonance lines. Such resonances were previously identified by means of dynamic micromagnetic simulations as uniform ($k=0$) translation DW resonance modes [19]. The resonance line at frequency $f_0=263$ MHz corresponds to a DW excitation localized within the Bloch part of the twisted DWs. This line can be excited by the small out-of-plane component of the pumping field. A second resonance line appears at $f_1=405$ MHz. This one is assigned to a DW excitation within the Néel parts of the DWs close to the film surfaces. This line is excited by the in-plane component of the pumping field. For $P = 25$ mW, the Bloch DW resonance line becomes asymmetric and a redshift of the resonance frequency is clearly observed. A much weaker redshift exists also for the Néel DW resonance frequency. In addition, the spectrum reveals a new weak resonance line at $f_0/2$. For $P = 50$ mW, the amplitude of this resonance at $f_0/2$ is significantly increased. From the DW resonance spectra recorded at multiple intermediate values of microwave power, the minimal power value for the appearance of the resonance at $f_0/2$ is estimated around $P_{m,1/2} = 5$ mW.

3.1.2 In-plane field spectra

To further clarify the origin of the signal revealed at half the frequency of the fundamental Bloch DW resonance, the DW resonance spectra have been measured for a few values of a DC magnetic field H_x applied along the stripe domain direction and for a fixed input microwave power $P = 30$ mW. Figure 3 shows the field evolution of the fundamental Bloch DW resonance (Fig. 3 (a)) and the one of the resonance at half the frequency of the Bloch DW resonance (Fig. 3(b)). The field dependence of the resonance frequency normalized by its value in the linear regime for both magnetic resonances is displayed in Fig. 3(c). For the fundamental Bloch DW resonance, a linear field variation of the resonance frequency is observed in agreement with previously reported data [20]. In the framework of the oscillator harmonic model, this behavior is explained by the decrease of the DW mass in conjunction with the increase of the restoring force constant (diminishing value of the stripe period [21]) for increasing in-plane magnetic field. The very similar linear variation of the resonance frequency with the magnetic field strength for the resonance at $f_0/2$ consolidates the hypothesis of a resonant magnetic excitation associated with collective DW oscillations.

3.2 Quantitative microwave power dependences

3.2.1 Fundamental DW resonances

Let us consider the Bloch DW resonance. Figure 4(a) displays the evolutions of the reduced resonance frequency and the reduced resonance linewidth as a function of the input microwave power P . The resonance frequency (resp. resonance linewidth) at a given power P is normalized by its low-power value ($P = 10^{-1}$ mW, linear regime). Several comments can be drawn. (i) The nonlinear redshift of the resonance frequency for increasing P values

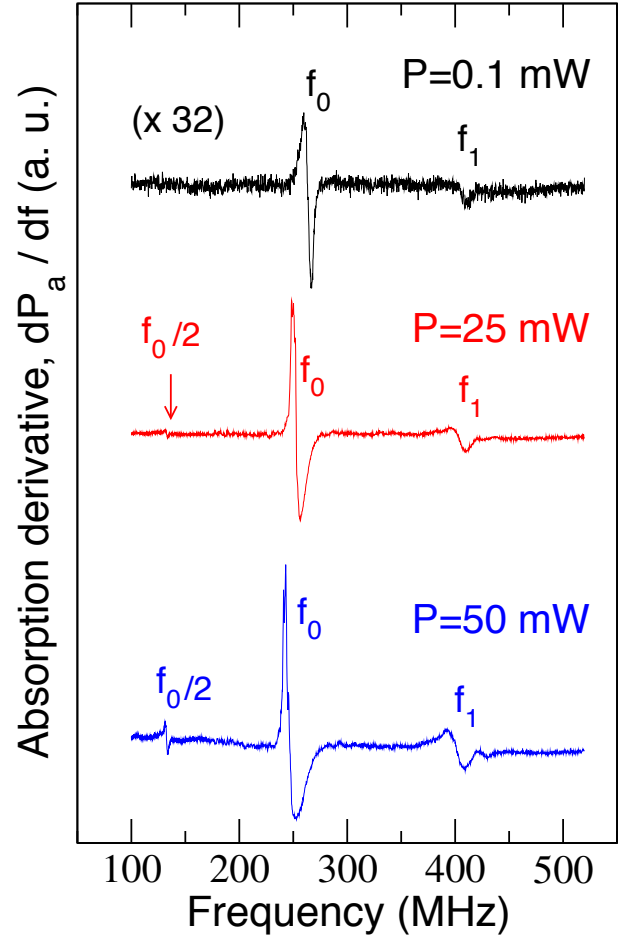


Figure 2. Experimental zero-field microwave power absorption spectra for three values of the input microwave power $P=0.1$ mW (linear regime), 25 mW and 50 mW. The amplification factor is labeled in the parentheses. The resonance frequency for the fundamental Bloch DW resonance and the Néel DW resonance are located at f_0 and f_1 , respectively. The $1/2$ subharmonic Bloch DW resonance appears at $f_0/2$

is significant and reaches 8% for $P=200$ mW. (ii) The resonance linewidth is increased for increasing P values according to a quadratic law above $P=5$ mW. For $P=200$ mW, the resonance linewidth is enhanced by a factor 1.8 with respect to the linear regime. Such power evolutions have been previously reported and nicely reproduced by micromagnetic simulations including a nonlinear damping parameter [9] for a sample with similar magnetic parameters except a slightly larger value of the saturation magnetization. (iii) The power absorption at resonance first increases rapidly with P and then saturates at $P_s = 50$ mW (Fig. 4(b)). It should be remarked that P_s is greater than the minimal power value for the appearance of the subharmonic resonance at $f_0/2$ ($P_{m,1/2} = 5$ mW).

Let us now move on the Néel DW resonance. Figure 5(a) shows the experimental power dependences for the reduced resonance frequency and the reduced linewidth. Similarly to the case of the Bloch DW resonance, a nonlinear redshift of the resonance frequency is observed for

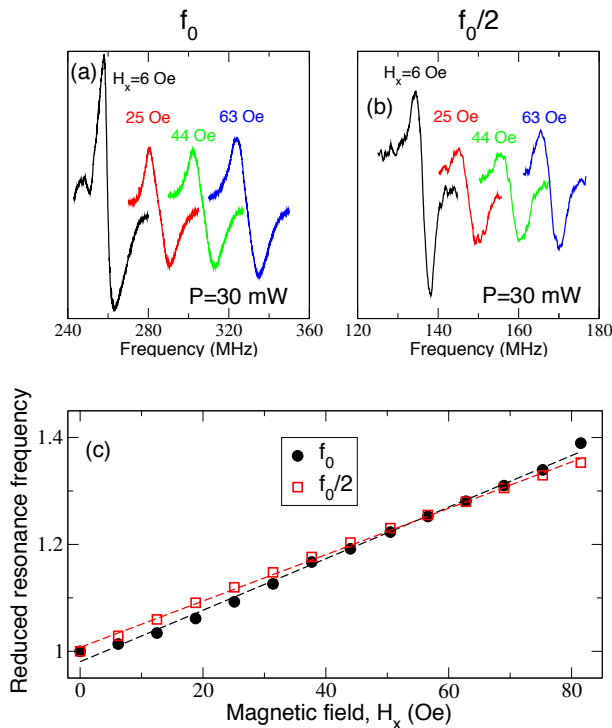


Figure 3. Experimental in-plane magnetic field dependence of the nonlinear DW resonances. (a) Fundamental DW resonance, (b) subharmonic Bloch DW resonance at $f_0/2$. The input microwave power is fixed at $P = 30$ mW. (c) In-plane field dependence for the reduced resonance frequencies of fundamental and subharmonic DW resonances. The resonance frequencies are normalized by those at zero-field. The dashed lines correspond to linear regressions.

increasing P values. However, the amplitude of variation is much weaker. The resonance frequency is reduced by around 1% at $P=200$ mW. The resonance linewidth first increases with P and then saturates for $P \approx 90$ mW. A decreasing trend of the resonance linewidth occurs for $P \geq 125$ mW. The amplitude of the power absorption at resonance displays a quite similar power dependence, the power saturation being nevertheless slightly upshifted (Fig. 5(b)). It should be remarked that the saturation of the power absorption for the Néel resonance ($P_s = 125$ mW) exceeds the one for the Bloch DW resonance ($P_s = 50$ mW) occurring at a lower frequency. On the other hand, the slight decreases of the resonance linewidth and the power absorption at resonance for $P \geq 125$ mW may be correlated with the emergence of a new resonance line (see the subsidiary line at 425 MHz for the DW spectrum at $P = 50$ mW in Fig.2) whose origin remains unknown at the moment.

3.2.2 1/2 Subharmonic Bloch DW resonance

Figure 6(a) shows the microwave power evolution of the DW spectra for the subharmonic of the Bloch DW resonance at $f_0/2$. The resonance lines are well-defined and narrow. For $P=25$ mW, the peak-to-peak linewidth for the

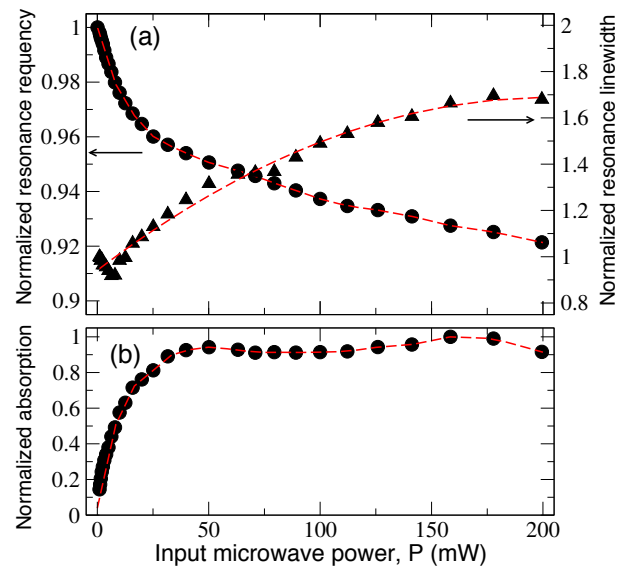


Figure 4. Experimental microwave power dependence for the fundamental Bloch DW resonance. (a) Reduced DW resonance frequency and reduced DW resonance linewidth as a function of the input microwave power P . The resonance frequency and the resonance linewidth are normalized by those in the linear regime ($P = 10^{-1}$ mW). (b) Reduced microwave power absorption at resonance as a function of P . The amplitude of the microwave power absorption is normalized by its maximum value. The dashed lines are guides to the eyes.

subharmonic at $f_0/2$ is 2.3 MHz compared to 7 MHz for the Bloch DW resonance at the same microwave power. The power dependences of this subharmonic line depart from those observed for the fundamental DW resonances. First, there is no resonance frequency shift up to $P=80$ mW. Then, a redshift of the resonance frequency accompanied with a monotonous variation of the power absorption at resonance for increasing P are evidenced. The maximum value of this redshift is around 3% at $P=150$ mW (Fig. 6(b)). The resonance linewidth is found nearly constant up to $P=150$ mW (Fig. 6(c)). The power dependence of the amplitude of the power absorption at resonance is displayed in (Fig. 6(d)). The amplitude of the power absorption increases nearly quadratically with P . For $P > 150$ mW the signal becomes distorted which prevents a quantitative analysis.

4 Theoretical analysis

A DW wave theory in the linear regime was developed by Slonczewski for parallel stripe domains in the large perpendicular anisotropy limit [22]. The DW dynamics is described by the Slonczewski's equations resulting from the integration of the Landau-Lifshitz-Gilbert equation over the DW width. The two degrees of freedom are: q , the DW displacement along the DW normal (y axis) and ψ the azimuthal angle of the magnetization evaluated at the middle of the DW from the elongation direction of the stripe domains (x axis). In the general case, q and ψ depend on the z coordinate along the film thickness.

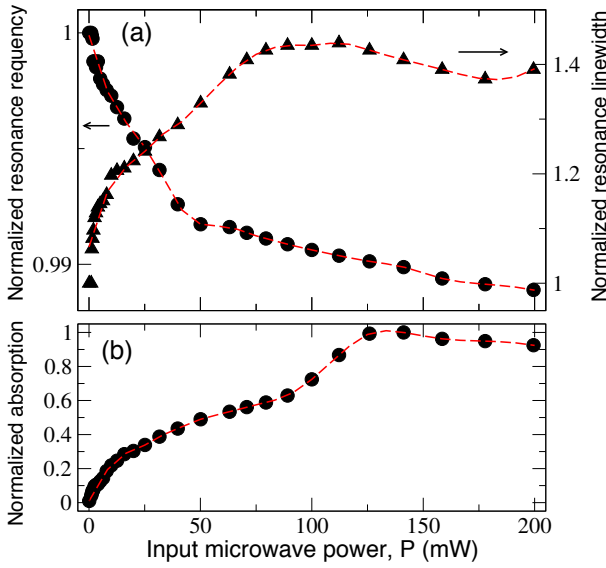


Figure 5. Experimental microwave power dependence for the Néel DW resonance. (a) Reduced DW resonance frequency and reduced DW resonance linewidth as a function of the input microwave power P . (b) Reduced microwave power absorption at resonance as a function of P . The normalization rules are the same as in Fig. 4. The dashed lines are guides to the eyes.

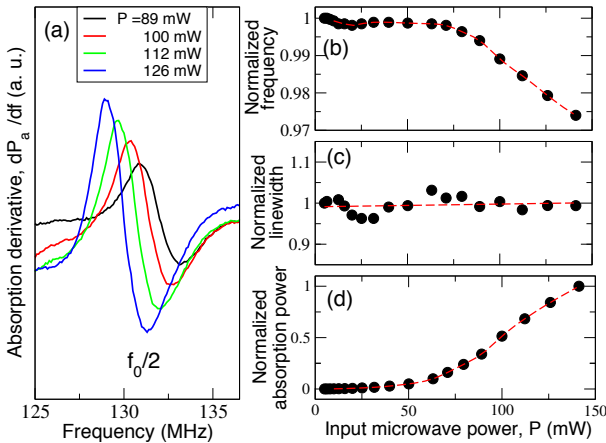


Figure 6. Experimental microwave power dependence for the 1/2 subharmonic Bloch DW resonance. (a) DW resonance spectra around $f_0/2$ for three values of the input microwave power. Input microwave power dependence for the resonance frequency (b), the resonance linewidth (c) and the power absorption at resonance (d) of the subharmonic signal at $f_0/2$. The normalization rules are the same as in Fig. 4. The dashed lines are guides to the eyes.

For small-amplitude oscillations about the equilibrium state, the linearized Slonczewski's equations are solved assuming a wave-like form for the dynamical variables with a two-dimensional (2D) in-plane wave vector (parallel and perpendicular to the stripe direction). It leads to an eigenmode equation and the eigenfrequencies can be computed as functions of the 2D DW wave vector. This theory has been used to identify the available collective DW modes existing at half the frequency of

the fundamental DW pumping mode that can be operative in the three-DW-magnon process [11]. However, such a process requires to excite the fundamental DW pumping mode and to detect the 1/2 subharmonic DW resonance separately which is in contrast with our experimental frequency sweeping procedure. Furthermore, this theory is restricted to small-amplitude DW oscillations.

As a first approach to analyze our experimental results, a simplified model has been considered based on the nonlinear Slonczewski's equations. The following assumptions have been made: (i) An array of a pure Bloch DW is considered. (ii) This array is excited by an oblique pumping field with an in-plane component δh_x parallel to the DW direction (x -axis) and an out-of-plane component δh_z . (iii) The pumping field has a harmonic time dependence with a pulsation ω . (iv) Only the dynamics of the uniform collective Bloch DW mode is analyzed. (v) The kinetic nonlinearity associated with a change of the DW structure is predominant with respect to the potential nonlinearity [23]. The Slonczewski's equations are then given by :

$$\dot{\psi} + \alpha\Delta_0^{-1}\dot{q} = \gamma\left(-\frac{k}{2M_s}q + \delta h_z\right), \quad (1)$$

$$\dot{q} - \alpha\Delta_0\dot{\psi} = 2\pi\gamma\Delta_0 M_s \sin 2\psi + \frac{\pi\gamma\Delta_0}{2}\delta h_x \sin\psi, \quad (2)$$

where the overdot denotes a time derivative, α is the Gilbert damping parameter, Δ_0 is the Bloch DW width parameter defined as $\Delta_0 = (A/K_u)^{1/2}$ and k is the restoring force constant due to the magnetostatic energy of the stripe domain structure [24].

The Slonczewski's equations are solved using a perturbation method based on the power expansion of the dynamical variables [25]:

$$\begin{aligned} q &= q_1 + q_2 + \dots, & q_1 \gg q_2 \gg \dots \\ \psi &= \psi_1 + \psi_2 + \dots, & \psi_1 \gg \psi_2 \gg \dots \end{aligned} \quad (3)$$

To the first order in q , ψ , δh_x , and δh_z , the Slonczewski's equations are:

$$\dot{\psi}_1 + \alpha\Delta_0^{-1}\dot{q}_1 = \gamma\left(-\frac{k}{2M_s}q_1 + \delta h_z\right), \quad (4)$$

$$\dot{q}_1 - \alpha\Delta_0\dot{\psi}_1 = 4\pi\gamma\Delta_0 M_s \psi_1. \quad (5)$$

By introducing: $\delta h_z = \delta h_z^0 \frac{e^{i\omega t} + e^{-i\omega t}}{2}$, and assuming the responses in the form: $\psi_1 = \psi_1^0 \frac{e^{i\omega t} + e^{-i\omega t}}{2}$ and $q_1 = q_1^0 \frac{e^{i\omega t} + e^{-i\omega t}}{2}$, the solutions are given by :

$$\psi_1^0 = \frac{i\omega}{D_1} \gamma \delta h_z^0, \quad (6)$$

$$\frac{q_1^0}{\Delta_0} = \frac{i\omega\alpha + 4\pi\gamma M_s}{D_1} \gamma \delta h_z^0, \quad (7)$$

where

$$D_1 = -\omega^2 + \omega_0^2 + i\alpha\omega\Delta\omega_0. \quad (8)$$

The resonance pulsation ω_0 is given by:

$$\omega_0^2 = 2\pi\gamma^2\Delta_0k, \quad (9)$$

and the frequency resonance linewidth is expressed by:

$$\Delta\omega_0 = \gamma(4\pi M_s + \frac{k\Delta_0}{2M_s}). \quad (10)$$

We obtain the well-known result that the DW displacement is induced only by the out-of-plane component of the pumping field and possesses a unique resonance at $\omega = \omega_0$.

To the second order in q , ψ , δh_x , and δh_z , the Slonczewski's equations are:

$$\dot{\psi}_2 + \alpha\Delta_0^{-1}\dot{q}_2 = \gamma(-\frac{k}{2M_s}q_2), \quad (11)$$

$$\dot{q}_2 - \alpha\Delta_0\dot{\psi}_2 = 4\pi\gamma\Delta_0M_s\psi_2 + \frac{\pi\gamma\Delta_0}{2}\delta h_x\psi_1. \quad (12)$$

The second term in the righ-hand side of Eq. 12 appears as an effective driving term which depends both on δh_x and ψ_1 and, consequently, oscillates at 2ω .

By introducing: $\psi_2 = \frac{\psi_2^0}{2} \frac{e^{2i\omega t} + e^{-2i\omega t}}{2}$ and $q_2 = \frac{q_2^0}{2} \frac{e^{2i\omega t} + e^{-2i\omega t}}{2}$, the solutions are given by :

$$\psi_2^0 = -\frac{\pi}{4} \frac{(2i\omega\alpha + \frac{\gamma k\Delta_0}{2M_s})}{D_2} \frac{i\omega}{D_1} \gamma\delta h_z^0 \gamma\delta h_x^0, \quad (13)$$

$$\frac{q_2^0}{\Delta_0} = -\frac{\pi}{2} \frac{\omega^2}{D_2 D_1} \gamma\delta h_z^0 \gamma\delta h_x^0, \quad (14)$$

where

$$D_2 = -4\omega^2 + \omega_0^2 + i\alpha\omega\Delta\omega_0. \quad (15)$$

Two main comments can be made. First, the second-order response requires the simultaneous presence of the two components of the pumping field. Second, q_2^0 and ψ_2^0 exhibit two resonance frequencies at $\omega = \omega_0$ and $2\omega = \omega_0$.

The power absorption is then computed by means of the general expression :

$$P_a = \langle \int_V dV \delta\mathbf{h} \cdot \frac{\partial\delta\mathbf{m}}{\partial t} \rangle_t, \quad (16)$$

where $\delta\mathbf{h}$ and $\delta\mathbf{m}$ are the total driving field and the total dynamic magnetization, respectively.

Using the relation between δm_z and the displacement q : $\delta m_z = \frac{4M_s}{P_0}q$, the expressions of the power absorption $P_{a,i\alpha}$ with $i = 1, 2$ and $\alpha = x, z$ are given by :

$$P_{a,1z} = \frac{2M_s}{P_0} \omega \Im(q_1^0) \delta h_z^0 \quad (17)$$

$$P_{a,2z} = \frac{4M_s}{P_0} \omega \Im(q_2^0) \delta h_z^0 \quad (18)$$

$$P_{a,2x} = \frac{\pi M_s}{32} \omega |\psi_1^0|^2 \Im(\psi_1^0) \delta h_x^0 \quad (19)$$

Figure 7 illustrates the total absorption derivative spectrum computed using Eqs 17, 18 and 19 for $\delta h_x^0 = 5$ Oe and $\delta h_z^0 = 2.5$ Oe. The computed spectrum reproduces the

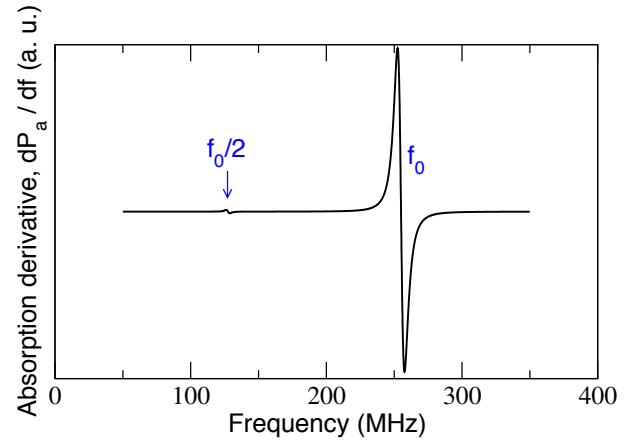


Figure 7. Zero-field absorption derivative spectrum computed from Eqs.17, 18 and 19. The magnetic parameters are those reported in Sec. 2 except $\alpha=0.006$. The sample is excited by an oblique pumping field with an in-plane component δh_x along the stripe direction and an out-of plane component δh_z . $\delta h_x^0 = 5$ Oe and $\delta h_z^0 = 2.5$ Oe.

onset of the subharmonic resonance at $f_0/2$. The amplitude ratio between the Bloch DW resonance and its 1/2 subharmonic is representative of the experimental data for the selected values of δh_x^0 and δh_z^0 .

However, it should be noted that these field values would correspond to an experimental input microwave power in the Watt range using a simple description of a straight microstrip reflection line. This power range is far in excess of our maximal experimental value $P_{max}=200$ mW. This suggests that other mechanisms contribute to the high level of the subharmonic resonance at $f_0/2$ for high microwave powers.

5 Summary and perspectives

Despite the relative simplicity of this magnetic texture, the stripe domain pattern possesses a rich and complex nonlinear translational DW excitation spectrum. In the present work, this excitation spectrum has been experimentally investigated by means of broadband FMR measurements at zero-field and in the presence of an in-plane DC magnetic field for increasing values of the input microwave power. The exciting field configuration corresponds to an oblique pumping field with the in-plane component parallel to the stripe domain direction and an out-of-plane component. For a low-level microwave power (linear regime), the uniform translational DW resonances (fundamental Bloch and Néel DW resonances) are detected. Increasing the input microwave power results in a redshift of the resonance frequency and a line broadening of these fundamental DW resonances, the amplitude of the redshift depending of the frequency position of the DW resonance line. In addition, a subharmonic resonance at half the frequency of the fundamental Bloch DW resonance has been detected and has been studied in detail. This narrow subharmonic signal appears from a moderate input microwave power and displays some salient features

(no redshift up to a critical microwave power, no power dependence of the resonance linewidth, a nearly quadratic variation of its amplitude at resonance for increasing microwave power) which contrasts with the power dependence of the fundamental DW resonances. An analytical model based on the nonlinear Slonczewski's equation and taking into account the oblique pumping field configuration enables us to reproduce semi-quantitatively the experimental results. Some perspectives can be drawn to follow up this work. From the theoretical viewpoint, a general description of the collective translational DW resonances in the nonlinear regime through 3D dynamic micromagnetic simulations would be of primary interest to go further in the interpretation of the experimental results. From the experimental side, zero-field broadband FMR measurements at higher microwave power levels could be suggested. For instance, preliminary measurements at $P=250$ mW indicate the presence of the $1/3$ subharmonic Bloch DW resonance whose features would deserve to be in-depth investigated. Lastly, it could be fruitful to explore the nonlinear translational DW resonances in garnet films with various magnetic parameters and to highlight how these parameters affect the nonlinear power dependences of the spectra.

References

- [1] U. Ebels, L.D. Buda, K. Ounadjela, P.E. Wigen, *Spin Dynamics in Confined Magnetic Structures I* (Springer, Berlin, 2002)
- [2] W.J. B. E. Argyle, J.C. Slonczewski, *J. Appl. Phys.* **54**, 3370 (1983)
- [3] J.M. Winter, *Phys. Rev.* **124**, 462 (1961)
- [4] J.F. Janak, *Phys. Rev.* **134**, A411 (1964)
- [5] Y. Henry, D. Stoeffler, J.V. Kim, M. Bailleul, *Phys. Rev. B* **100**, 024416 (2019)
- [6] J. Lan, W. Yu, R. Wu, J. Xiao, *Phys. Rev. X* **5**, 041049 (2015)
- [7] N. Vukadinovic, J.B. Youssef, *Phys. Rev. B* **100**, 224423 (2019)
- [8] W. Jantz, B. Argyle, J.C. Slonczewski, *IEEE Trans on Magn.* **16**, 657 (1980)
- [9] N. Vukadinovic, J.B. Youssef, N. Beaulieu, V. Castel, *Phys. Rev. B* **92**, 214408 (2015)
- [10] H. Suhl, *J. Phys. Chem. Solids* **1**, 209 (1957)
- [11] B. Argyle, J.C. Slonczewski, W. Jantz, J.H. Spreen, M.H. Kryder, *IEEE Trans on Magn.* **18**, 1325 (1982)
- [12] J.H. Spreen, B.E. Argyle, *Appl. Phys. Lett.* **38**, 930 (1981)
- [13] J.C. Slonczewski, *J. Magn. Magn. Mater.* **31-34**, 663 (1983)
- [14] E. Schlömann, J.J. Green, U. Milano, *J. Appl. Phys.* **31**, S386 (1960)
- [15] F. Guo, L.M. Belova, R.D. McMichael, *Phys. Rev. B* **699**, 1 (2014)
- [16] T. Brächer, P. Pirro, B. Hillebrands, *Physics Reports* **89**, 104422 (2017)
- [17] B.E. Argyle, J.C. Slonczewski, E.A. Giess, *Appl. Phys. Lett.* **24**, 396 (1976)
- [18] H.L. Gall, N. Vukadinovic, J. Ostorero, J.M. Desvi-gnes, *J. Magn. Magn. Mater.* **84**, 229 (1990)
- [19] N. Vukadinovic, J.B. Youssef, M. Labrune, *Phys. Rev. B* **66**, 132418 (2002)
- [20] M. Ramesh, E. Jedryka, P.E. Wigen, M. Shone, *J. Appl. Phys.* **57**, 3701 (1985)
- [21] W.F. Druyvesteyn, J.W.F. Dorleijn, P.J. Rijnierse, *J. Appl. Phys.* **44**, 2397 (1973)
- [22] J.C. Slonczewski, *J. Magn. Magn. Mater.* **23**, 305 (1981)
- [23] A.K. Zvezdin, N.E. Kulagin, V.G. Red'ko, *Phys. Met. Metallogr.* **45**, 3 (1979)
- [24] J. Morkowski, H. Dötsch, P.E. Wigen, R.J. Yeh, *J. Magn. Magn. Mater.* **25**, 39 (1981)
- [25] A.G. Gurevich, G.A. Melkov, *Magnetization Oscillations and Waves* (CRC Press, Boca Raton, Florida, 1996)